The Iraqi Journal For Mechanical And Material Engineering, Vol.11, No.1, 2011

STUDYING OF FLAPS AND SLATS EFFECTS ON IMPROVING THE AERODYNAMIC FORCES OF THE WINGS

Ali K. Al-Abadi
Manufacturing Operation Dept
Al-Kawarizmi College of Engineering
University of Baghdad

ABSTRACT:

A numerical method was used for calculation the pressure distribution and then finding aerodynamic forces to give an estimation for the high- lift systems effect on two-dimensional airfoil for an inviscid incompressible flow (panel method), the computational method investigated experimentally. The study focused on flap and slat effects on the aerodynamic forces at the wings as two of the important items of the high lift systems.

Experimental study was made with suction type low-speed wind tunnel for an airfoil of (NACA 0015) supported with leading edge slat and trailing edge flap. The effective forces of lift and drag were measured by two components balance. Different angles of attack $(-4, 0, 4, 8 \& 12)^o$ and different flap angles $(0, 10, 20 \& 30)^o$ were chosen with and without slat, variable air velocities (8, 12, 16 & 20)m/s were applied. The computational results compared with experimentally measured data.

Key words (Flap, High-Lift, Airplane, wings, panel method)

دراسة تأثير الشرائح واللوحات على تحسين قوى الديناميكية الهوائية للأجنحة

الخلاصة

تم اجراء استخدام طريقة عددية لحساب توزيع الضغط ومن ثم ايجاد القوى الايروديناميكية لاعطاء تخمين عن تاثير انظمة تحسين الرفع لنموذج ريشة ثنائية البعد ولجريان غير لزج لاانضغاطي، وتم تحقيق الطريقة الحسابية تجريبيا. وقد ركزت الدراسة على تاثير الجنيحات الخلفية والشرائح الامامية على القوى الايروديناميكية المؤثرة على الاجنحة كاهم متغيرين لانظمة تحسين الرفع.

الدراسة التجريبية تمت باستعمال نفق هوائي ساحب واطيء السرعة واستعمال نموذج ريشة نوع (NACA 0015) مجهزة بشريحة امامية وجنيح خلفي. القوى المؤثرة على الجناح (الرفع والكبح) تم قياسها باستخدام الميزان الثنائي. تم تغيير زوايا الهجوم للجناح $(-4, 0, 4, 8 \& 12)^o$ وكذلك زوايا الجنيح مختلفة $(0،10،20 \& 30)^o$ مع وجود وبدون الشريحة الامامية بالاضافة الى تطبيق سرع هواء متعددة (8, 12, 16 & 20)m/s.

INTRODUCTION:

Wings designed for airplane with high lift to drag ratio; must be also designed for an efficient take-off and landing. Take-off and landing distances are influenced directly by aircraft stalling speed, with lower stall speeds requiring deceleration that result shorter field lengths. Many options could make enhancement to the wings lift such as boundary layer control, wing area control and wing weight.

It is always possible to reduce stall speed by increasing wing area, but it is not desirable to cruise with long distance of extra wing area where the associated weight and drag are increases, area that is only needed for a few minutes till the take-off or landing happened. Since the stalling speed is related to wing parameters, where as Robert W. Fox, Alan T. McDonald, 1998:

$V_{stall}=(2W/(S\rho C_{Lmax}))^{1/2}$
S= Wing area
W= weight
C_{Lmax}= Maximum lift coefficient
ρ=density

So, it is possible to reduce stalling speed by reducing weight, increasing air density, increasing wing C_{Lmax}, or increasing wing area.

The latter parameter is the most interesting. Where; it is usually more efficient to include movable leading and/or trailing edges so that one may obtain good high speed performance while achieving a high C_{Lmax} at take-off and landing.

The increase in C_{Lmax} is associated with an increase in chord length provided by motion along the flap track or by a rotation axis that is located below the wing and in front of wing for slat fig (1).

Hak-Tea Lee and Ilan M. Kroo, 2004, made a computational investigation for wings with flaps of 90^{o}'s named miniature trailing edge (MiTEs). Numerous experiments and computational simulations have been conducted for 2-D airfoil with miniature flaps, and the study focused on examines the 3-D aerodynamics of MiTEs by using an incompressible Navier-Stockes flow solver to investigate the span wise distribution induced lift along the airfoil, in addition, the effect of gaps between the flaps was examined.

Carl J. Wenzinger and Francis M. R., 1964, Made an extensive investigation in the NACA 7- by 10-foot wind tunnel of spoiler, deflector, and slot types of lateral-control device on wing with full-span split and slotted flaps, and determined the static rolling and yawing moments for all devices tested, a spoilers alone on the wing upper surface were unsatisfactory unless located near the trailing edge, while deflectors on lower surface appeared to have insufficient power when operating alone but were beneficial in combinations with spoilers, and suggested a plug-type spoilers-slot aileron appeared to be the most satisfactory device investigated for use a full-span slotted flap.

A numerical technique (panel method) used to design these complex systems; however, the prediction of CLmax by direct computation is still difficult and unreliable. The most comprehensive numerical solution is due to Hess & Smith, 1966 & Smith, 1975, by solving two-dimensional airfoil in steady incompressible flow by using source and vortex distribution on the surface with using Kutta condition. The method discrete vortex shedding from the trailing with strength equal to the negative vortex strength of the airfoil, the approach gives good behavior of the wake and loads.

The current study focused on the wing area control; slats and flaps systems as one of the important options for high-lift systems.

The main aim of a high- lift system is a high C_{Lmax}; although, it is desirable to maintain low drag at take-off and landing.

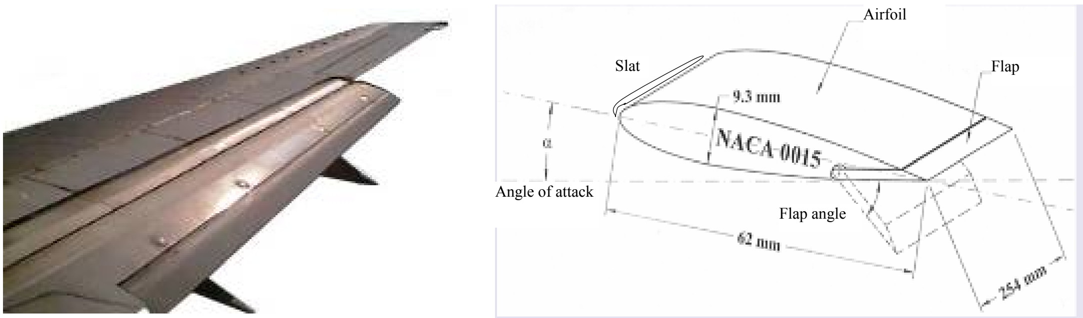

Fig (1) Wing with Slat and rectangular flap

MATHEMATICAL MODEL:

Momentum Integral Equation

The momentum θ equation first derived by von karman, 1921,

$$\frac{d\theta}{dx} + \frac{\theta}{V_e}(2 + H)\frac{dV_e}{dx} = \tfrac{1}{2}c_f$$

In which the shape factor H could be stated as;

$$H \equiv \delta^*/\theta$$

C_f is the skin friction coefficient in which defined as;

$$c_f \equiv \frac{\tau_w}{\frac{1}{2}\rho V_e^2}$$

τ_w=wall shear

Equation (1) contain many unknowns like θ,H and Cf. a variety methods to solve the equation (1) are exist. Many involved assumptions for velocity profile u or data fitting is used.

Boundary Layer

Head's method is based on the concept of an entrainment velocity. If δ(x) is the boundary-layer thickness, the volume rate of the flow Q within the boundary layer at x is;

$$Q(x) = \int_0^{\delta(x)} u\, dy \qquad (2)$$

The entrainment velocity E is the rate at which Q increases with x.

$$E = \frac{dQ}{dx} \qquad (3)$$

Some idea as to the physical significance of E can be gained from fig. (2)

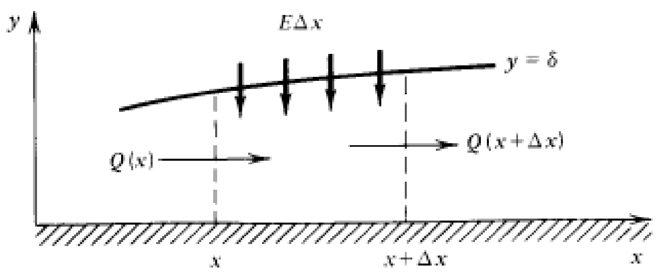

Fig.(2): concept of entrainment.

Combining equation (2) with the below equation of displacement thickness of the boundary layer, in which stated as follows,

$$\delta^*(x) \equiv \int_0^{\infty}\left[1 - \frac{u(x, y)}{V_e(x)}\right] dy \qquad (4)$$

To get,

$$\delta^* = \delta - \frac{Q}{V_e}$$

And from equation (3) we find;

$$E = \frac{d}{dx} V_e(\delta - \delta^*) \tag{5}$$

This could be rewritten as;

$$E = \frac{d}{dx}(V_e \theta H_1)$$

Where

$$H_1 \equiv \frac{\delta - \delta^*}{\theta} \tag{6}$$

Head's assumed that the dimensionless entrainment velocity E/Ve depend only on H1 and that H1, in turn, is a function of H=δ*/θ. Cebeci and Bradshaw, 1977, fit several sets of experimental data with the following formulas:

$$\frac{1}{V_e}\frac{d}{dx}(V_e \theta H_1) = 0.0306(H_1 - 3)^{-0.6169} \tag{7}$$

$$\begin{aligned} H_1 &= 3.3 + 0.8234(H - 1.1)^{-1.287} && \text{for} \quad H \le 1.6 \\ &= 3.3 + 1.5501(H - 0.6778)^{-3.064} && \text{for} \quad H > 1.6 \end{aligned} \tag{8}$$

Equations (1), (7) and (8) represent three equations among the four unknowns θ, H, H1 and Cf. head's completes the set with ludwieg-tillman skin-friction.

$$c_f = 0.246 \times 10^{-0.678H} \mathrm{Re}_\theta^{-0.268} \tag{9}$$

Which derived simply by fitting data available from various experimental studies, according to White, F. M., 1991, this formula is accurate to -10% to +10%.

Boundary Layer Growth Along an Airfoil

To perform a calculation, one needs first of all, the distribution Ve(x) of velocity of a non-viscous fluid along the airfoil surface. Potential panel method was used to calculate velocity distribution along the airfoil surface detail of panel method stated in the next section.

The x of boundary layer equation is not a Cartesian coordinate but is measured along the airfoil surface, with x=0 locating the stagnation point. I^{th} point at which the boundary is to be calculated and at which the potential-flow velocity is Ve; These points are distributed along the surface of airfoil by cosine low, which concentrate the computation points near the stagnation point, where Ve varies most rapidly. To find the gradient velocity at calculation points, it could be done by fitting a parabola to the values of Ve at three successive points; that is, by finding constants a, b and c such that as Katz J., Plotkin A,1991:

$Ve=a+bx+cx^2$

At three adjacent points, we then differentiate the formula with respect to x and evaluate the results at the point under study. It must be at first put the value of θ at stagnation point which is obtained from equation below;

$$\tilde{\theta}(0) = \sqrt{\frac{0.075}{\mathrm{Re}\, \tilde{\tilde{V}}_0}}$$

Where

$$\tilde{\tilde{V}}_0 \equiv \frac{d\tilde{V}_e}{d\tilde{x}}(0)$$

To integrate the two differential equations (1) and (7), a second order Runge-Kutta method is used. For separation point, equation (8) always give a positive C_f, so it could not be predict separation by locking for zero value of Cf. the simplest alternative criterion for turbulent separation is based on the computed value of H. thus, when H>2.4, the boundary layer has separated Kline, S. J. et al., 1983. This criterion is usually adequate, since H to increase rapidly near separation anyway.

Panel Method

Much more powerful approaches can be based on distributions of sources and vortices or doublets. The flow tangency boundary condition is applied and satisfied on the body surface; also these singularities should be distributed on the body surface rather than on the chord line or any other line within the body.

It is simply stated by distribution source and vortex singularities on the body surface at straight lines called Panels as shown in fig.(3).

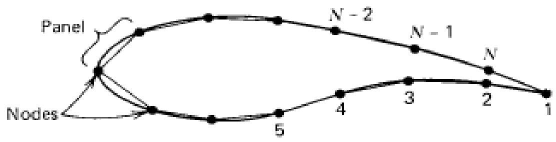

Fig.(3) panels for 2-D airfoil

EXPERIMENTAL PROCEDURES

The sub-sonic suction type wind tunnel fig.(4), with 30 *30 cm test section area and maximum air speed of 26 m/s was used, the airfoil of NACA 0015 (symmetrical airfoil with maximum lift coefficient at 15% of the chord) fig(1), supported with leading edge slat and trailing edge flap was fixed on two balance component.

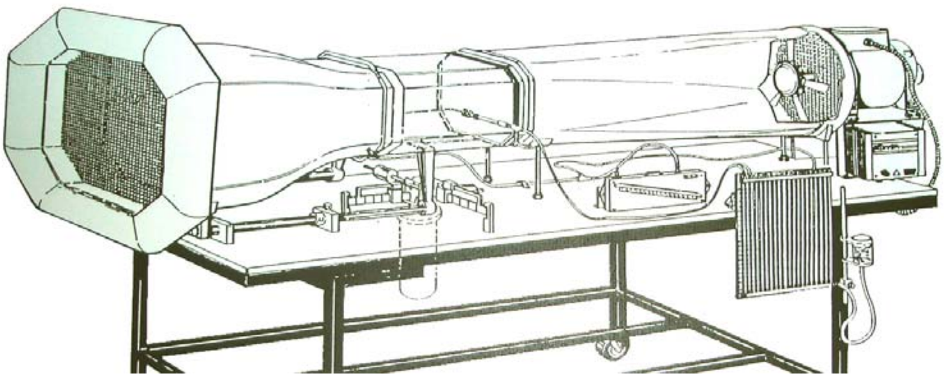

Fig. (4) wind tunnel with its accessorie

First the airfoil supported over the two balance component and fixing the attack angle (AOA) to -4^o and the flap angle to 0^o. The effected aerodynamics forces (Lift and Drag) were measured. The previous steps repeated for AOA=0^o, and again for other attack angles (4, 8, 12)^o, and all for flap angle =0^o. Repeat all angles of attack (-4, 0, 4, 8 & 12)^o for flap angle 10o, then again repeated for other flap angles (20, 30)^o. Then measurements were taken for different angles of attack for different flap angel without slat. All for multi air speeds (8, 12, 16 & 20) m/s were applied.

All aerodynamic forces were measured with two-component balance system of maximum balance rating-lift of 7 N and maximum balance rating-drag of 2.5 N with sensitivity of ±0.01 N.

Lift and drag forces were measured with different angle of attack, with and without slat and with different flap angles

RESULTS AND DISCUSSION

Figure (5) shows the comparison between the variation of the theoretical and the experimental Lift and Drag coefficients with angle of attack variation for Re=33067, and flap angle=0, 10^o, 20^o, 30^o respectively, the fig shows the effect of flaps clearly, where with the flap at the trailing edge of airfoil causes an increasing of airfoil area and camber that leads to increase lift coefficient.

Figures (6, 7, 8) shows the same variation of Lift and Drag coefficients for Re=49600, Re=66133, Re=82667 respectively

As it seems the lift and drag coefficients increases with the increment of air velocity (Reynolds No.) and also with the increment of attack angle because the frontal area increases.

Also figs show the variation of drag and lift coefficients with the variation of angle of attack for different air velocities, and flap angles, without slat. It shows that the lift coefficient increases with the increment of angle of attack and air velocity till the angle of attack between (12^o-14^o) then the lift decreases due to stall (when the lift force is less than the airfoil weight).

All figs show a good convergence between theoretical and experimental results.

Also Figs show comparison between experimental and theoretical drag and lift coefficients, although the deviation between experimental and theoretical increase with the increment of attack angle but, it show acceptable comparing between them.

Fig (9) shows a comparison between lift and drag coefficient results for the airfoil with and without slat for air velocity=12 m/s and flap angle=0. It seems that with slat at the leading edge the lift increases due to the increment of the effective radius of the leading edge and also, the slat prevents flow separation by opening a slot that helps keep air flow attached to the wings upper surface which make lift force increases, and comparison also shows that the slat effect increases with the increments of attack angle.

With the slat at the front rear of the airfoil, the resulting data have the same trend for all curves but with little increment for lift and drag coefficient due to the effect of slat.

Figure (10) shows Lift coefficient versus angle of attack for airfoil with and without flap where (a) data from [1] for airfoil NACA 23012 and (b) data from recent work for airfoil NACA 0015, only trend comparison between the two figs could be done due to different profile, also it shows the stall angle for both.

CONCLUSIONS

1. Flaps cause an increasing of airfoil area and camber that leads to increase lift and drag coefficient, that increasing depends on increment of flap angle.
2. Increment of chord Reynolds no. also increase lift and drag coefficients.
3. The deviation between experimental and theoretical increase with the increment of attack angle, and in general it show acceptable comparing between them.
4. Slats at the leading edge of an airfoil increase the lift, and the slat effect increases with the increments of attack angle.

REFERENCES

Robert W. Fox, Alan T. McDonald, "Introduction to Fluid Mechanics", John Wiley & Sons, 1998.

Hak-Tae Lee and Ilan M. Kroo, "Computational investigation of wings with miniature trailing edge control surfaces", papar, AIAA, 2004.

Carl J. Wenzinger and Francis M. R, "wind-tunnel investigation of spoiler, deflector, and slot lateral- control devices on wings with full-span and slotted flaps", NACA report no. 706, 1964.

Hess J. L., Smith A. M. O., "Calculation of Potential Flow about Arbitrary Bodies", Progress in Aeronautical Science, Vol. 8, Pp. 1-138, Pergamon Press Oxford, 1966.

Hess J. L., "Review of Integral-Equation Techniques for Solving Potential-Flow Problems with Emphasis on Surface-Source Method", Comput. Methods in Appl. Mechanics and Eng., 5, 145-196, 1975.

Schlichting, H., Boundary-Layer theory, 7th ed., New York: McGraw-Hill, 1979.

Cebeci, T., and Bradshaw, P., Momentum transfer in Boundary Layer. McGraw-Hill, Washington, D.C. (1977).

White, F. M.,viscous fluid flow, 2nd ed. New York: Mc Graw-Hill, 1991.

Katz J., Plotkin A., "Low-Speed Aerodynamics from Wing Theory to Panel Methods", International Edition, McGraw-Hill, 1991.

Kline, S. J., Bardina, J. G., and Stawn, R. C., "Correlation of the Detachment of Turbulent Boundary Layers," AIAA J. 21, 68-73 (1983).

Alan Pope, John J. Harper, "Low-Speed Wind Tunnel Testing", John Wiley & Sons, 1966.

Morgan, H.L., Ferris, J.C., and McGhee, R.J., "A study of high-lift airfoils in the Langley low-turbulence pressure tunnel", NASA, July 1987.

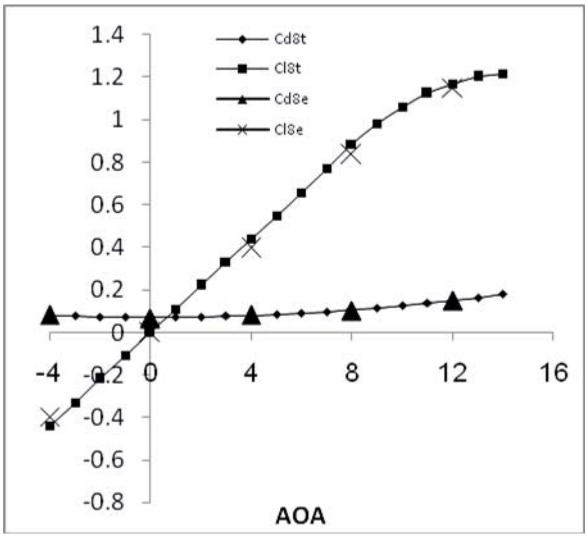

(a)

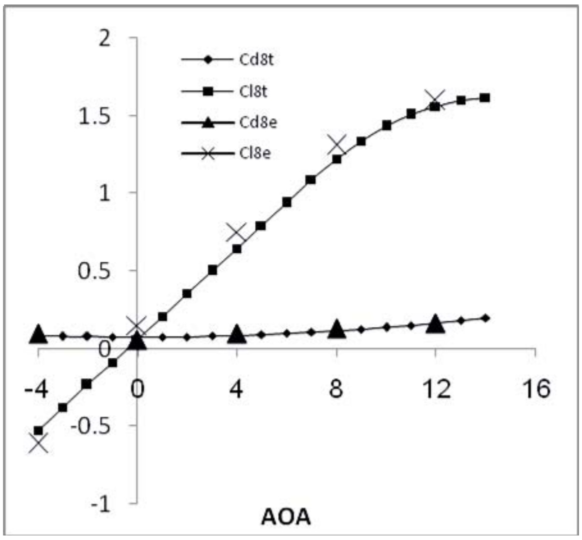

(b)

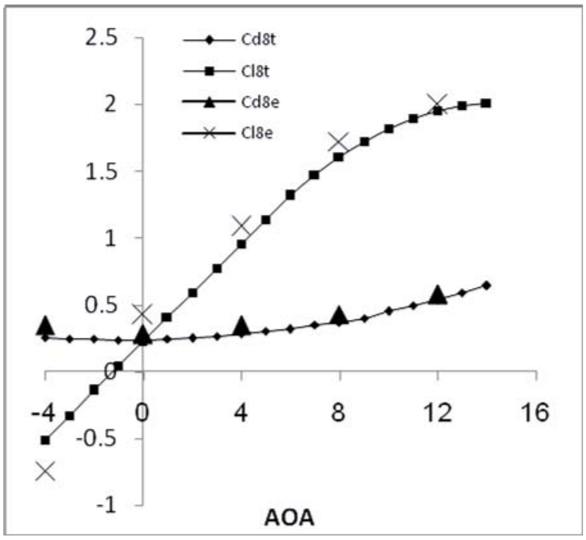

(c)

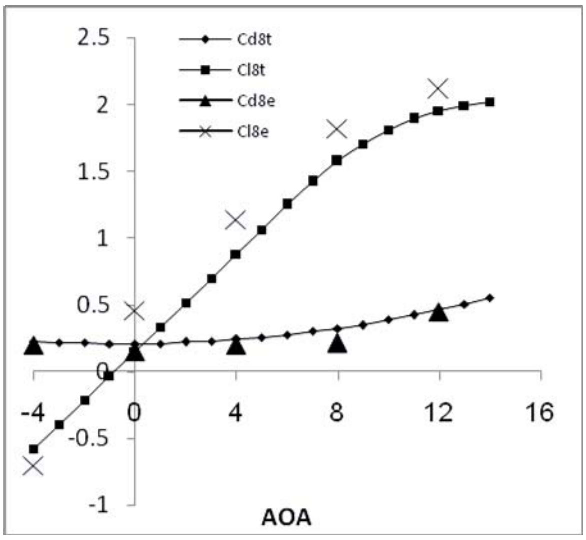

(d)

Fig.(5) Theoretical and Experimental Lift and Drag coefficients variations with angle of attack variation for Re=33067 (v=8 m/s), and flap angle=0, 10^o, 20^o, 30^o respectively.

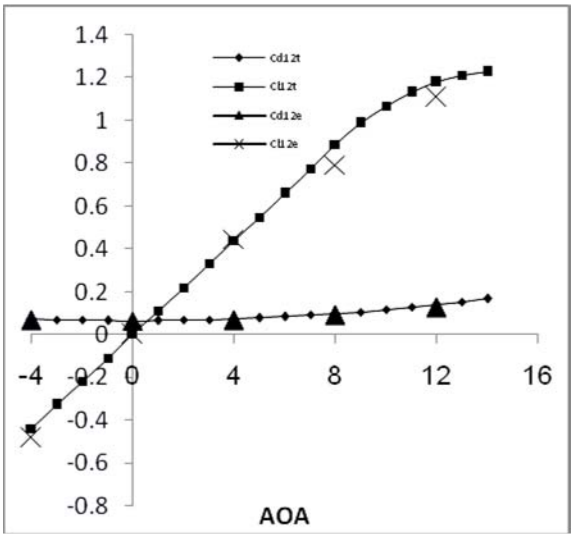

(a)

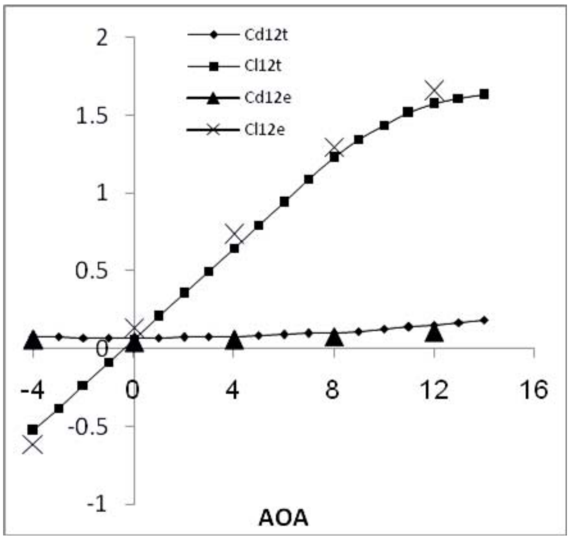

(b)

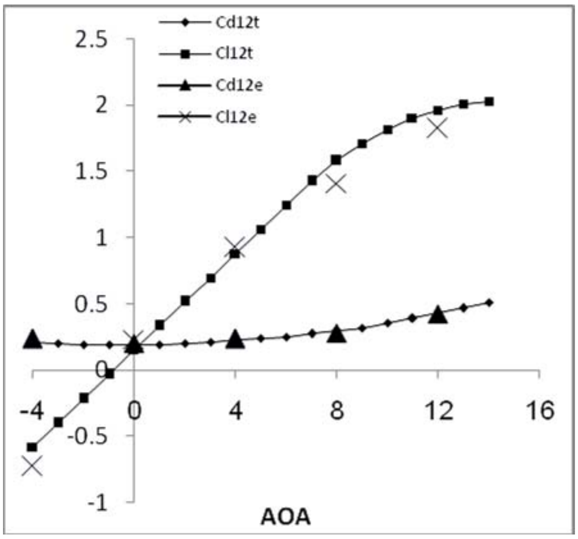

(c)

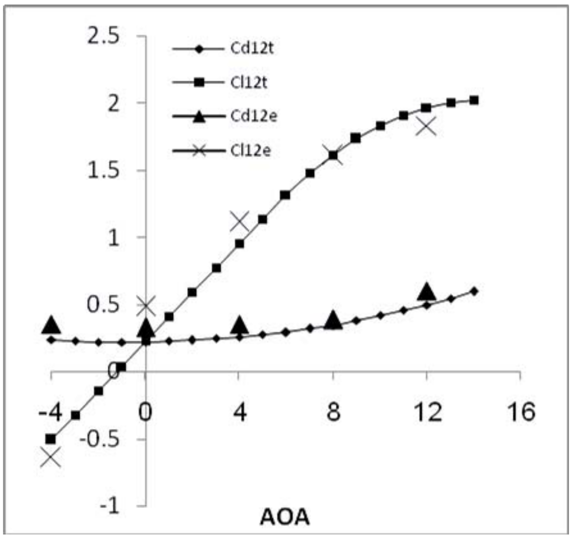

(d)

Fig.(6) Theoretical and Experimental Lift and Drag coefficients variations with angle of attack variation for Re=49600 (v=12 m/s), and flap angle=0, 10^o, 20^o, 30^o respectively.

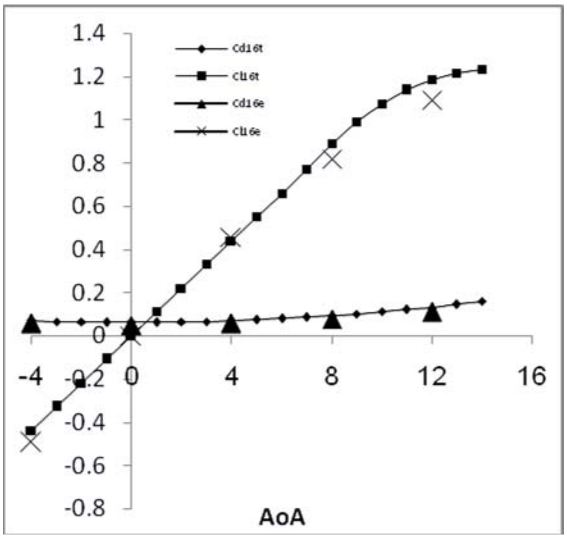

(a)

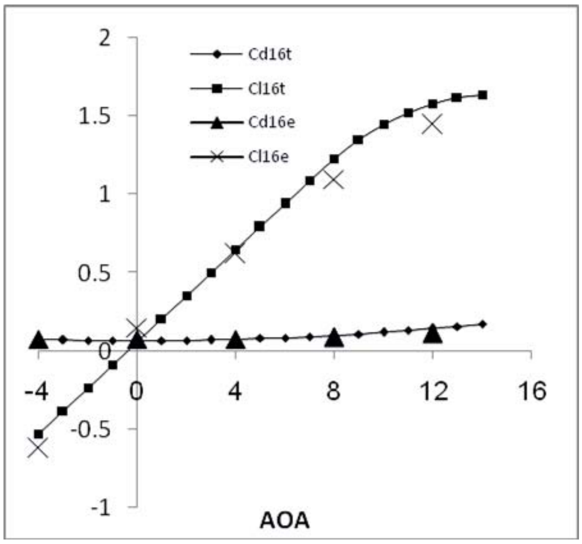

(b)

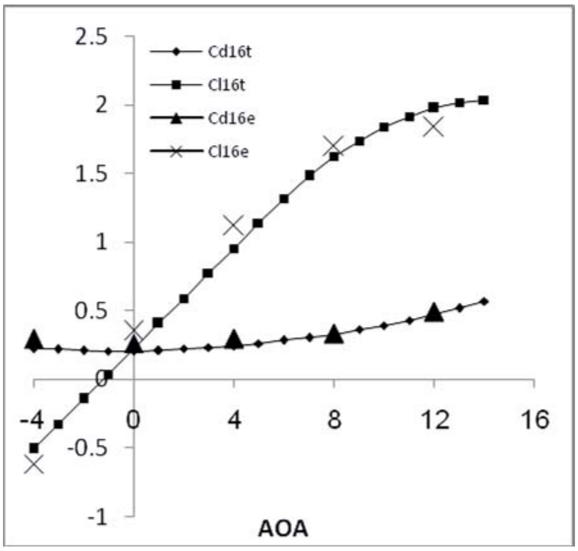

(c)

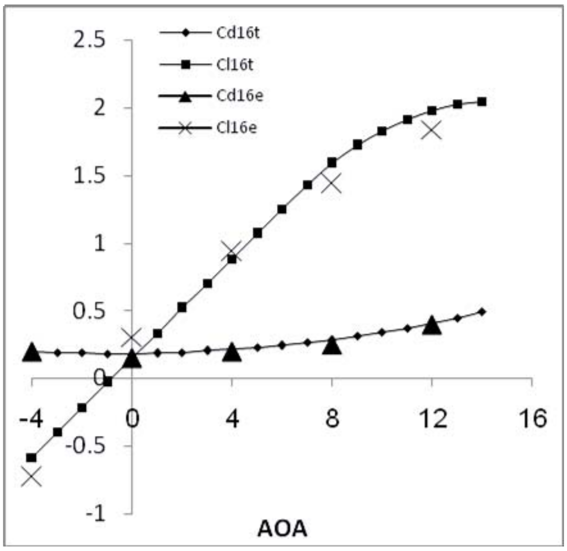

(d)

Fig.(7) Theoretical and Experimental Lift and Drag coefficients variations with angle of attack variation for Re=66133 (v=16 m/s), and flap angle=0, 10^o, 20^o, 30^o respectively.

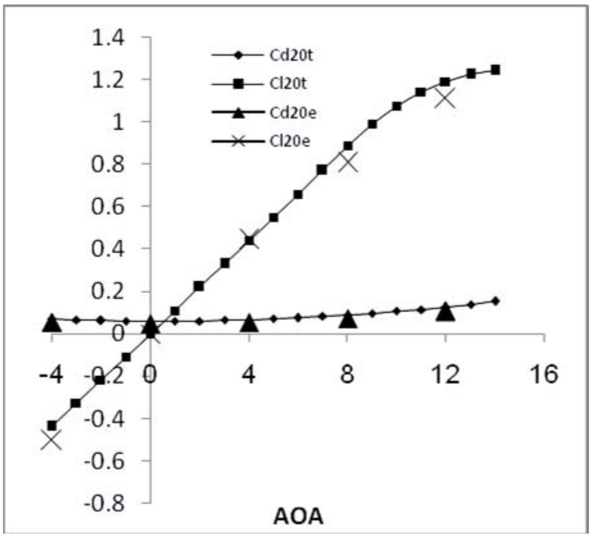

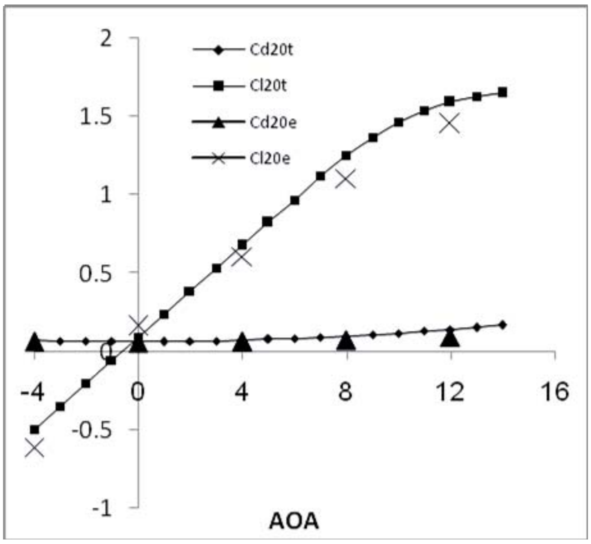

(a) (b)

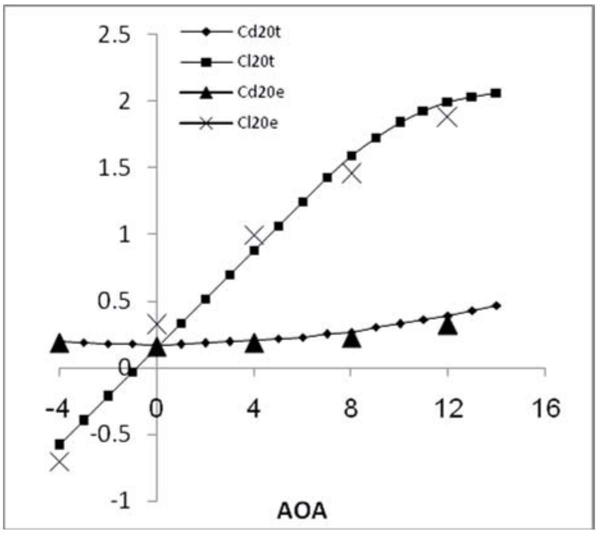

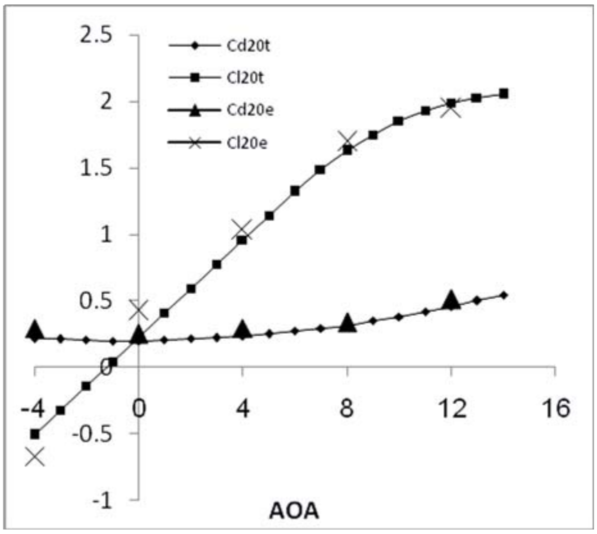

(c) (d)

Fig.(8) Theoretical and Experimental Lift and Drag coefficients variations with angle of attack variation for Re=82667 (v=20 m/s), and flap angle=0, 10^o, 20^o, 30^o respectively.

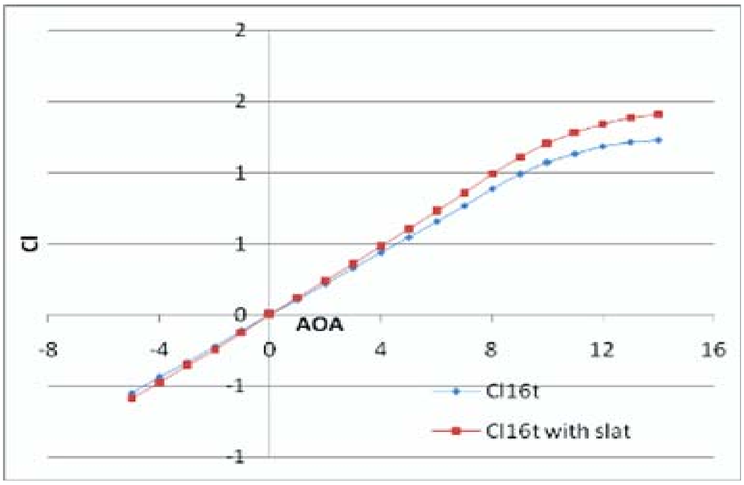

Fig (9-a) Lift coefficient Versus AOA for airfoil with and without slat and air velocity=12 m/s

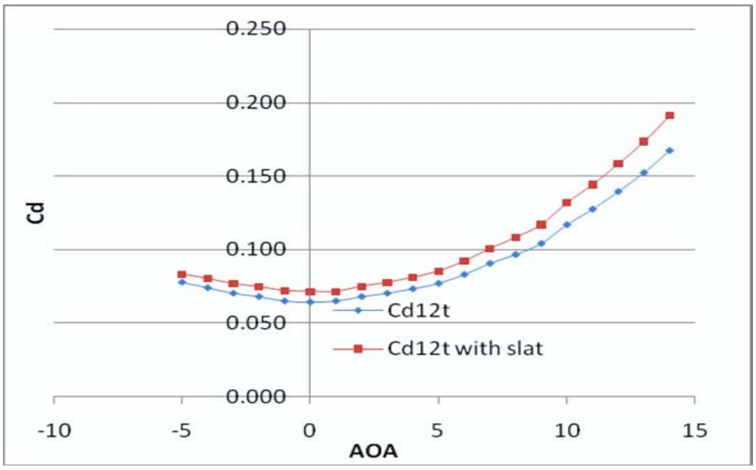

Fig (9-b) Drag coefficient Versus AOA for airfoil with and without slat and air velocity=12 m/s

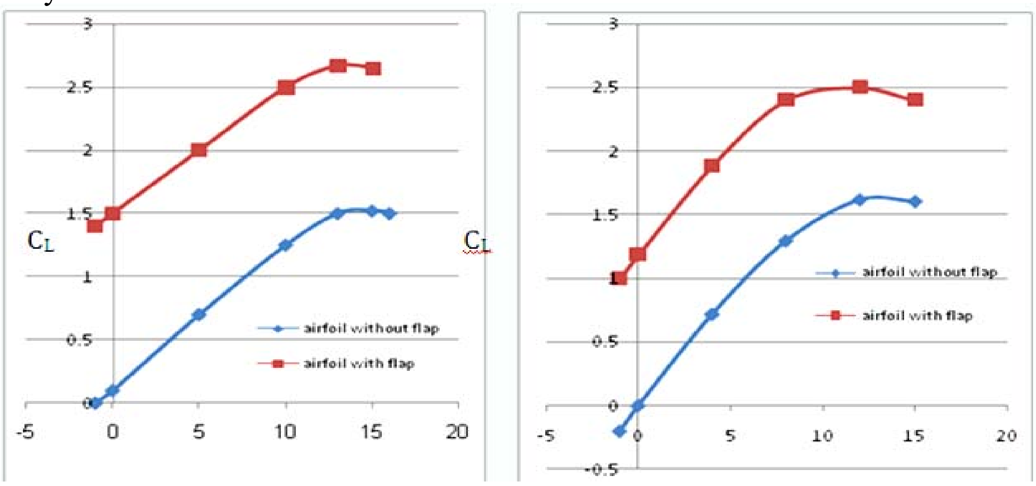

(a) *(b)*

Fig (10) Lift Coefficients versus AOA for airfoils with and without flap

(a) data from [1] for airfoil NACA 23012 and (b) data from recent work for airfoil NACA 0015